

PAPER • OPEN ACCESS

Optimization of UAV's Landing Longitudinal Control under Wind Disturbance

To cite this article: Wenhui Qu *et al* 2021 *IOP Conf. Ser.: Earth Environ. Sci.* **693** 012106

View the [article online](#) for updates and enhancements.

You may also like

- [Unmanned aerial vehicle fault diagnosis based on ensemble deep learning model](#)
Qingnan Huang, Benhao Liang, Xisheng Dai *et al.*
- [Cooperative navigation of unmanned aerial vehicle formation with delayed measurement](#)
Chenfa Shi, Zhi Xiong, Mingxing Chen *et al.*
- [A framework for improving UAV decision of autonomous navigation from training to application migration under perceptual uncertainty](#)
Yuanyuan Sheng, Huanyu Liu, Junbao Li *et al.*



ECS
The
Electrochemical
Society
Advancing solid state &
electrochemical science & technology

DISCOVER
how sustainability
intersects with
electrochemistry & solid
state science research

Optimization of UAV's Landing Longitudinal Control under Wind Disturbance

Wenhui Qu, Hanqi Zhang and Yiwei Dong*

School of Aerospace Engineering, Xiamen University.

Email: 272807031@qq.com, 642762950@qq.com, yiweidong@xmu.edu.cn

Abstract. Environmental factors have a great influence on the autonomous landing process of UAV. In order to enhance the environmental adaptability of UAV's landing control, this paper takes a certain high-speed UAV as the research object, analyzes the main causes of the error in UAV's landing under the wind interference, and puts forward the improvement measures. The object model was built under the Matlab/Simulink platform to simulate the closed loop control system of UAV's autonomous landing, and the Monte Carlo method was used to verify the robust performance of the control system in the presence of the wind interference. The simulation results show that the improved landing plan can effectively reduce the landing error of UAV under the wind interference and improve the landing accuracy and safety of UAV.

1. Introduction

Autonomous landing is one of the important methods of UAV recovery and also the key technology of UAV's control. High-speed UAV has high touchdown speed, so its landing control is more difficult. In order to ensure the safety of UAV's autonomous landing, tracking of the preset height and speed trajectory are required longitudinally, and aiming at the center line of the runway is required laterally^[1], so as to ensure that the UAV is grounded at a certain speed, subsidence rate and pitch angle. For the safe landing of UAV, it is necessary to design a reasonable landing trajectory^[2] combining the aerodynamic characteristics, fly environment, landing indicators and other parameters of UAV, and to design a landing control law with good stability and control accuracy^[3], in order to ensure the UAV can fly in strict accordance with the designed trajectory.

The certain high-speed UAV studied in this paper is shown in Figure 1. The take-off weight of the UAV is 500kg, the length of the fuselage is 5.23m, the wingspan is 3.24m, the wing area is 4.84m², and the take-off speed is 60m/s.



Figure 1. A high-speed UAV.

The UAV has completed the test flight verification. During the test flight, if there was a large wind interference during the landing period, the control effect of lifting speed in the lift section would be affected, thus affecting the precision and safety of landing. In this context, this paper studies the



longitudinal control during the landing process of UAV, optimizes the landing control plan, so as to enhance the adaptability of UAV's landing control to wind interference conditions and improve the precision and safety of UAV landing.

2. Landing Error Analysis

2.1. Introduction To Original Landing Control

The landing process of UAV is divided into four stages: approach stage, descending stage, pull-up stage and slipping stage, as shown in Figure 2.

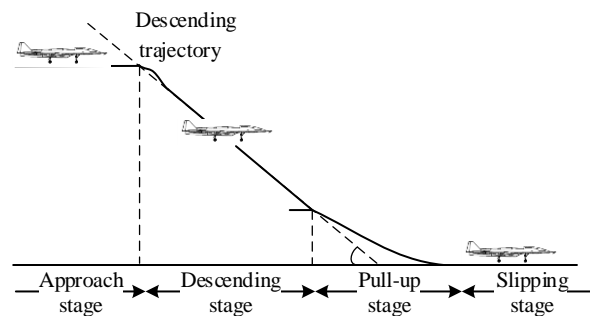


Figure 2. Schematic diagram of UAV landing trajectory.

After the UAV reaches the predetermined height and speed, it comes in level flight and switches to the descending stage by means of "Impact the descending trajectory extension cord". Track the descending path line in the descending stage, enter the pull-up stage after reaching the pull-up height, decelerate and reduce the height according to the pull-up trajectory, and touch the ground with a certain speed, subsidence rate and pitch angle. After the UAV touches the ground, it enters the slipping stage, turns off the engine, connects to the deviation correction control, and then decelerates to taxi until it stops at the runway. The design of landing trajectory is a reverse process, which needs to determine the attitude angle's range of touchdown according to the requirements of touchdown speed and lifting speed, and then determine the pull-up trajectory.

The descending stage can track the altitude profile, establish and stabilize the equivalent airspeed of UAV, and reduce or eliminate the altitude and velocity errors^[4].

The pull-up stage is the most important stage for autonomous landing of UAV, which determines whether UAV can land safely. The pull-up stage is designed based on the manned aircraft's exponential pull-up design method. The lift speed instruction is shown in Formula (1). The speed trajectory is designed by combining the gaussian pseudo-spectral trajectory optimization method.

$$\dot{H}(t) = -\frac{1}{\tau_H} H + \dot{H}_{jd} \quad (1)$$

In the Formula (1): τ_H is the exponential flattening curve time constant, \dot{H}_{jd} is the touch-ground lifting speed allowed by the UAV.

In the original landing plan, the aerodynamic characteristics and engine characteristics of the aircraft were taken into consideration comprehensively, and the trajectory angle of the steep descent was selected as $\gamma = -4^\circ$, level flight approaching speed was $V_0 = 80$ m/s, the speed of pull-up point was $V_1 = 61.7$ m/s, the touchdown speed was $V_2 = 50$ m/s, the height of pull-up point was $H_0 = 20.3$ m/s, $\tau_H = 5.5$, $\dot{H}_{jd} = -0.5$.

The control structure of UAV in landing stage is composed of inner loop and outer loop. The inner loop is the pitch angle control, which can increase the damping of the system, thus increasing the longitudinal stability of the system, and control the attitude at the same time. The outer loop is height

control or lifting speed control. In the descending stage, total energy control is adopted to realize height trajectory tracking. The control structure is shown in Figure 3. The lifting speed control is used in the pull-up stage to ensure that the touchdown speed is in a safe range. The control structure is shown in Figure 4.

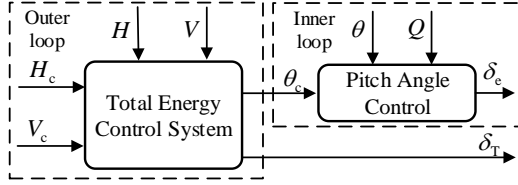


Figure 3. Height control structure diagram.

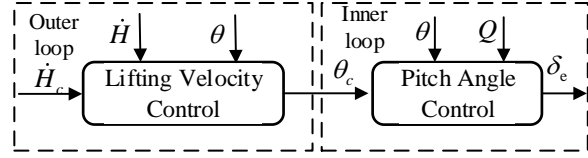


Figure 4. Lifting velocity control structure diagram.

In the above, H_c , H are altitude instruction and altitude respectively; V_c , V are speed instruction and speed respectively; \dot{H}_c , \dot{H} are lifting speed instruction and lifting speed respectively; θ_c , θ are pitch angle instruction and pitch angle respectively; Q is rate of pitch angle; δ_e is the elevator and δ_T is the engine throttle.

The lifting speed control^[5] is designed based on LADRC, and the control structure is shown in Figure 5. Pitch angle control is designed based on cascade active disturbance rejection method and is divided into pitch angle control circuit and pitch angle rate control circuit^[6] according to the principle of time scale separation. The control structure is shown in Figure 6.

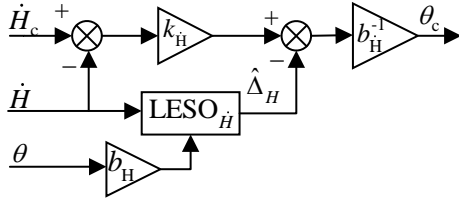


Figure 5. LADRC lifting speed control structure.

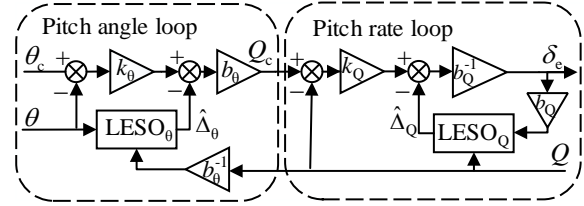


Figure 6. LADRC Pitch angle control structure.

In the above: k_H is lifting speed control coefficient; $\text{LESO}_{\dot{H}}$ is the second order linear extended state observer of the lifting speed (Linear extended state observer, LESO); $\hat{\Delta}_H$ is LESO's estimate of \dot{H} ; the control input gain is $b_H = 0.5\rho V^2 S C_{L\alpha} / m$; ρ is atmospheric density; S is the wing's area; $C_{L\alpha}$ is the derivative of lift coefficient with respect to angle of attack. LESO_{θ} , LESO_Q are LESO of pitch angle and LESO of pitch angle rate respectively; $\hat{\Delta}_\theta$ is LESO's estimate of θ , k_θ is pitch angle loop gain, and control input gain is $b_\theta = 1$; Q_c is pitch angle rate instruction; $\hat{\Delta}_Q$ is second order LESO's estimate of Q , k_Q is pitch angle rate control coefficient, and control input gain is $b_Q = 0.5I_y^{-1} \rho V^2 S c_A C_{M\delta_e}$; I_y is the moment of inertia about the Y-axis of the frame, c_A is the average aerodynamic chord length, $C_{M\delta_e}$ is the derivative of the pitching moment coefficient with respect to the elevator's deviation.

2.2. Influence of Wind Disturbance On Landing Simulation

The UAV uses total energy control to track altitude command and airspeed command in the descending stage, while the height control in the pull-up stage is disconnected, the lifting speed control and tracking lifting speed command is connected. According to the previous landing plan, the lifting speed track of the pull-up stage is fixed and changes with the height. However, because the tracking of the descending stage is the airspeed instruction, when there is wind interference, the airspeed and

ground speed will be inconsistent, resulting in the deviation of the lifting speed and the preset trajectory, thus affecting the landing state.

When the wind speed is 0m/s, 10m/s and -15m/s respectively, the UAV landing simulation results are shown in Table 1 and Figure 7.

Table 1. Comparison of touchdown states at different wind speeds.

Wind speed (m/s)	Forward distance (m)	Airspeed (m/s)	Pitch angle (°)	Lifting speed (m/s)
0	8.15	51.7	10.9	-0.53
10	51.97	49.86	11.8	-0.61
-15	-113.04	53.68	10.18	-0.46

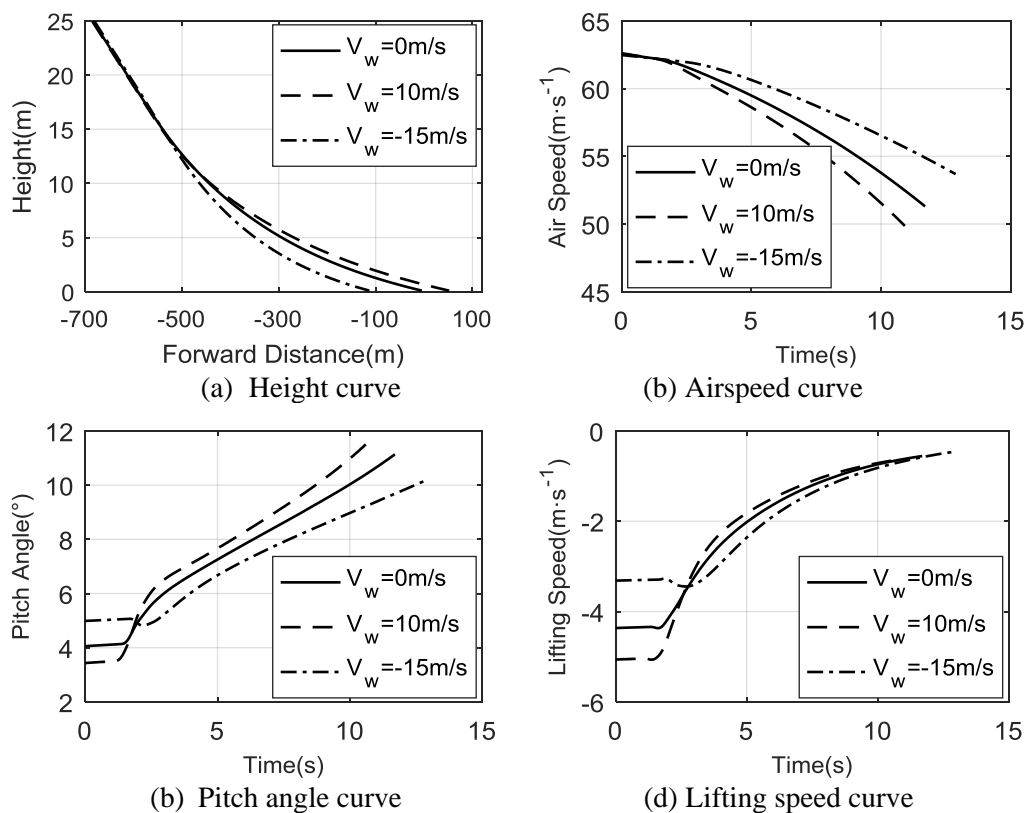


Figure 7. Simulation images of landing at different wind speeds.

It can be seen that the original landing plan:

1) When following wind, the ground speed is greater than the airspeed, and the initial lifting speed of the pull-up point is less than the design value. The lifting speed instruction makes the UAV directly pull up. The lifting distance is relatively long, and the UAV's landing point is moved backward;

2) When against the wind, the ground speed is less than the airspeed, and the initial lifting speed of the pull-up point is greater than the design value, which leads to that the lifting speed first decreases and then increases when entering the pull-up stage. The UAV first lowers its head and then raises its head. The ground speed is relatively small, the flying distance of the pull-up stage is relatively short, and its landing point is moved forward.

3. Optimization of Landing Plan

3.1. Optimization Plan

Due to the wind interference, there is a deviation between the initial lifting speed of the pull-up stage and the instruction of the lifting speed, which affects the touchdown state. Therefore, it is necessary to eliminate the deviation of the initial lifting speed. Considering the trajectory of the lifting speed is

$\dot{H}_c = -\frac{1}{\tau_H}H + \dot{H}_{jd}$, generally, keep touchdown lifting speed \dot{H}_{jd} constant, To change the initial lifting speed command, it is needed to change either the time constant τ_H or the pull-up point height H_0 . Considering that the velocity trajectory of the descending stage is obtained by the initial value and the terminal value according to the linear interpolation of the forward distance, if H_2 is directly changed, the distance of the descending stage will be affected, the velocity of the pull-up point will be changed, and the subsidence rate will also be affected, so the strategy of changing the time constant τ_H is adopted.

Making the initial lifting speed of the pull-up point be \dot{H}_0 , then the new time constant τ_{H1} of the pull-up trajectory is shown in Formula (2):

$$\tau_{H1} = \frac{-H_0}{\dot{H}_0 - \dot{H}_{jd}} \quad (2)$$

When the pull-up height is reached, the time constant is recalculated according to Formula (2), and then the new time constant is used to track the lifting speed trajectory, while other trajectories remain unchanged. Similarly, when the wind speed is respectively 0m/s, 10m/s and -15m/s, the UAV landing simulation results are shown in Table 2 and Figure 8.

Table 2. Comparison of touchdown states at different wind speeds (optimized plan).

Wind speed (m/s)	Forward distance (m)	Airspeed (m/s)	Pitch angle (°)	Lifting speed (m/s)
0	-33.58	52.10	10.83	-0.53
10	-35.74	52.31	11.81	-0.61
-15	-33.39	51.51	10.95	-0.46

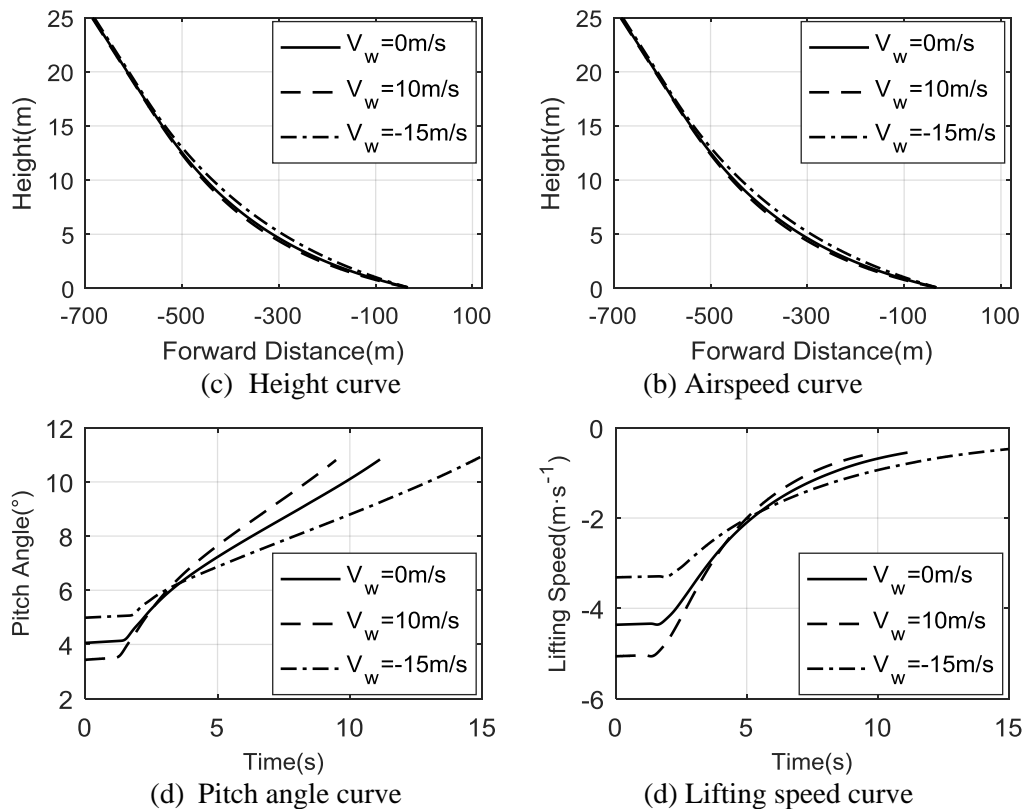


Figure 8. Simulation images of landing at different wind speed (optimized plan).

It can be seen that the optimized landing plan:

1) Under different wind speeds, the lifting speed curves are smoother, and there is no fluctuation at the pull-up point. The touchdown point, airspeed, pitch angle and lifting speed are close to those when there is no wind;

2) When following wind, the initial lifting speed is less than the design value, τ_{H1} decreases, and the time of pull-up stage decreases;

3) When against the wind, the initial lifting speed is greater than the design value, τ_{H1} increases, and the time of pull-up stage increases.

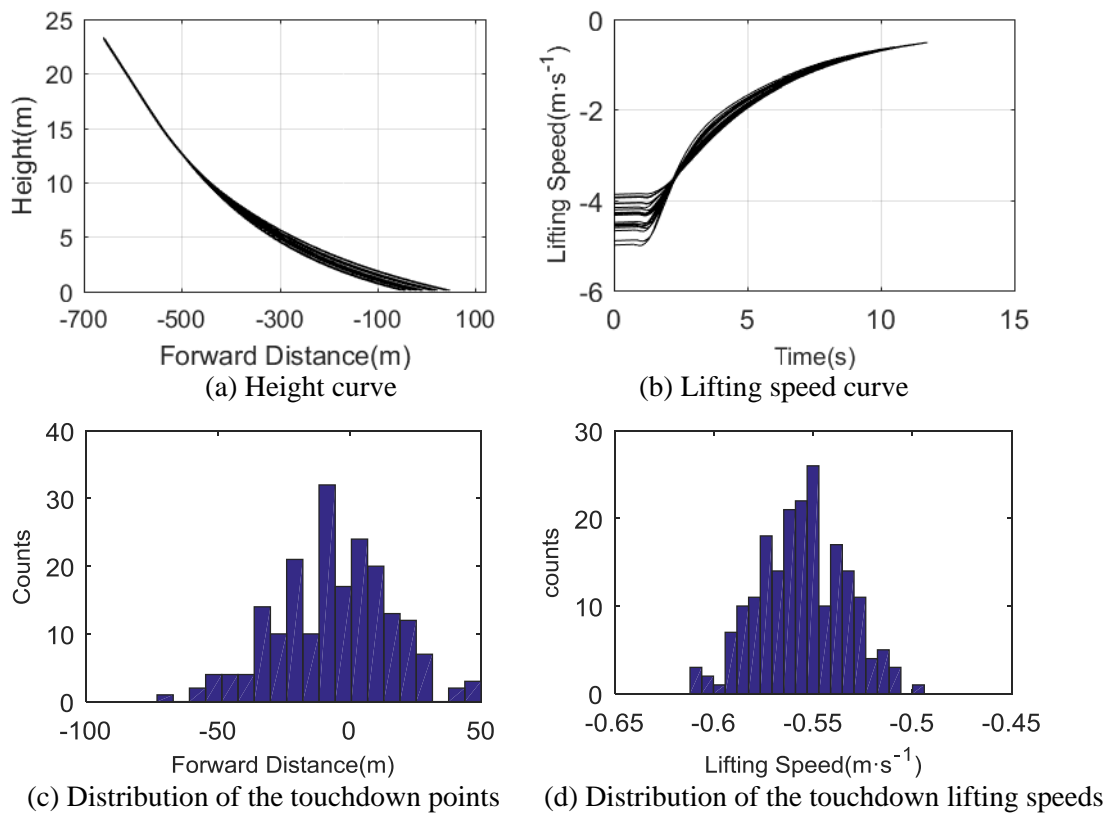
The optimized plan can effectively improve the tracking effect of the pull-up trajectory and reduce the deviation of the UAV landing point.

3.2. Monte Carlo Simulation

Monte Carlo method is used to verify landing simulation under wind disturbance, and the simulation effect of optimized landing plan under different wind speeds is investigated. The uncertainty range of wind disturbance is $\pm 10\text{m/s}$. Monte Carlo simulation was carried out for 200 times before and after optimization respectively. The simulation results are shown in Figure 9 and Figure 10, and the touchdown state is shown in Table 3.

Table 3. Comparison of the two plans in Monte Carlo simulation.

plans	/	Airspeed (m/s)	Pitch angle ($^{\circ}$)	Lifting speed (m/s)	Forward distance (m)
original	Range	49.96~52.83	10.51~11.76	-0.61~-0.49	-73.1~49.9
	The average value	51.28	11.15	-0.56	-5.94
	The standard deviation	0.50	0.22	0.022	21.75
optimized	Range	51.60~52.50	10.3~11.0	-0.6 ~ -0.5	-39.9 ~ -26.7
	The average value	51.9	10.87	-0.55	-31.7
	The standard deviation	0.18	0.05	0.017	2.55

**Figure 9.** Monte Carlo simulation results before optimization.

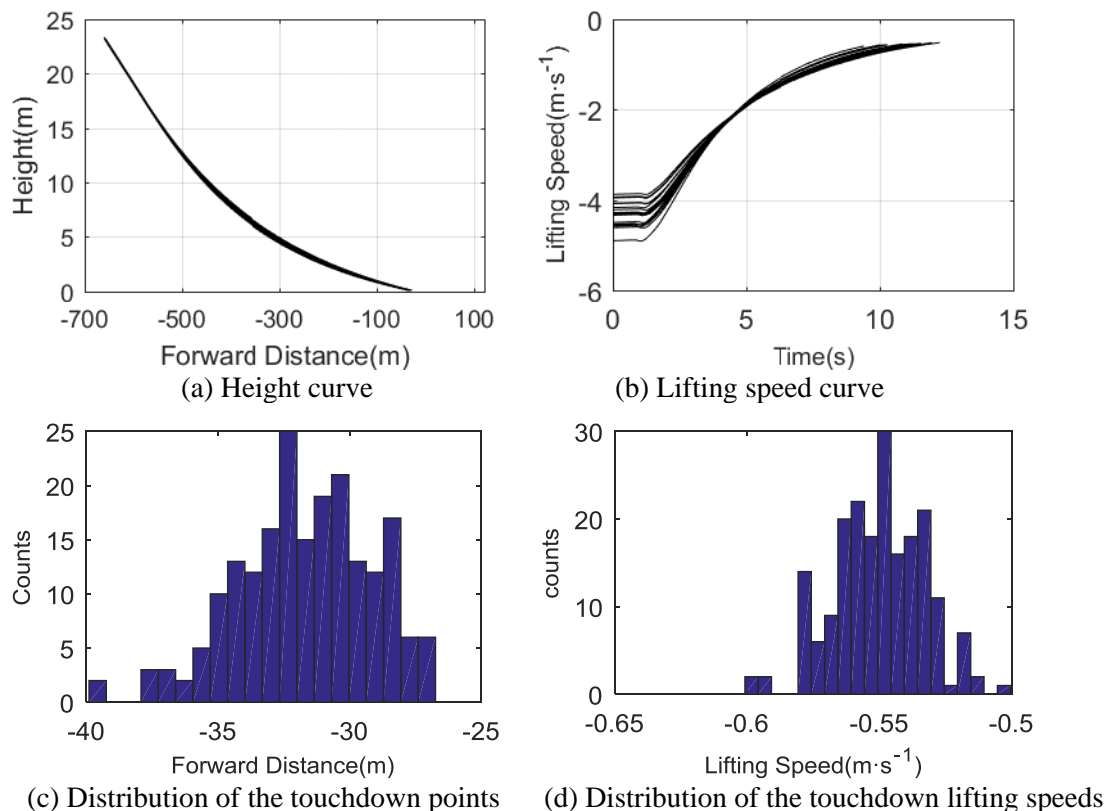


Figure 10. Monte Carlo simulation results after optimization.

It can be seen that the optimized landing plan has more concentrated distribution of touchdown airspeed, pitch angle, lifting speed and forward distance, smaller standard deviation, stronger anti-wind interference ability and stronger robustness.

4. Results

In this paper, the influence of wind disturbance on landing simulation is analyzed, and the landing plan is modified by modifying time constant method. Simulation results show that the improved landing plan can effectively reduce the landing error of UAV, meet the design requirements, and enhance the robustness of the control system.

5. References

- [1] Rudolf Brockhaus 1999 *Flight control* (Beijing: National Defense Industry Press)
- [2] Feixiang Zhu, Yong Gao, Hao Meng 2017 Design and simulation of UAV autonomous landing control system based on reference trace *Journal of Naval Aeronautical and Astronautical University* **32**(5) pp 463-468
- [3] Gao Lili 2017 Conceptual design and research on control technology of autonomous landing for a fixed wing unmanned aircraft vehicle *Nanjing: Nanjing University of Aeronautics and Astronautics*
- [4] Lei Li, Yimin Huang, Chunzhen Sun 2014 On longitudinal control of landing for UAVs under complex conditions *Electronics Optics & Control* **21**(11) pp 62-65+99
- [5] Zhiqiang Gao 2003 Scaling and bandwidth-parameterization based controller tuning *Proceedings of the American Control Conference (Denver, Colorado: IEEE)* pp 4989-4996.
- [6] Yanxiong Wang 2017 Take-off and landing control for flying-wing unmanned aerial vehicle Xi'an: *Northwestern Polytechnical University*